

Exact Classification of Landau-Majorana-Stückelberg-Zener Resonances by Floquet Determinants

Sriram Ganeshan, Edwin Barnes, and S. Das Sarma

Condensed Matter Theory Center and Joint Quantum Institute, Department of Physics, University of Maryland, College Park, Maryland 20742, USA

(Received 15 July 2013; published 25 September 2013)

Recent experiments have shown that Landau-Majorana-Stückelberg-Zener (LMSZ) interferometry is a powerful tool for demonstrating and exploiting quantum coherence not only in atomic systems but also in a variety of solid state quantum systems such as spins in quantum dots, superconducting qubits, and nitrogen vacancy centers in diamond. In this Letter, we propose and develop a general (and, in principle, exact) theoretical formalism to identify and characterize the interference resonances that are the hallmark of LMSZ interferometry. Unlike earlier approaches, our scheme does not require any approximations, allowing us to uncover important and previously unknown features of the resonance structure. We also discuss the experimental observability of our results.

DOI: [10.1103/PhysRevLett.111.130405](https://doi.org/10.1103/PhysRevLett.111.130405)

PACS numbers: 03.65.Aa, 03.67.Ac, 07.05.Dz

Introduction.—Driven quantum two-level systems have been extensively studied since the advent of quantum mechanics. A new wave of interest in coherent two-level dynamics has arisen recently in the context of solid state quantum devices, where rapid progress in fabrication techniques has made it possible to observe the signatures of the coherent evolution of few-level quantum systems in a solid state environment. Perhaps the most striking signatures of quantum coherence in two-level systems are the interference patterns that appear in the final state probability when the system is coherently driven through an avoided crossing repeatedly. This physical process is known as Landau-Majorana-Stückelberg-Zener (LMSZ) interferometry [1–5]. First observed in atomic and optical systems [6–8], LMSZ interferometry has recently been demonstrated in few-level solid state systems including nitrogen vacancy centers in diamond [9–11], spins in quantum dots [12–15], charge qubits [16], and superconducting qubits [17–19]. The abundance of applications to quantum computing, especially with superconducting qubits, has been largely responsible for the recent revival of this field. In all these manifestations, LMSZ interferometry has served as a powerful tool in measuring coherence times, mapping out the energy level diagram, and executing a target quantum evolution.

These advances in the experimental implementations of LMSZ interferometry have in turn spurred recent progress in the theoretical understanding of this phenomenon in a variety of contexts [5,20–31]. Generally the type of periodic driving field considered most often in LMSZ experiments, simple monochromatic driving, cannot be solved exactly. Numerous approximate approaches have therefore been developed in the literature to treat this case including the rotating wave approximation [21], perturbative Floquet theory [24,32,33], and the adiabatic impulse model [5,20]. These approaches involve either replacing the

monochromatic field with a different but related driving protocol that is more amenable to an analytical treatment or expanding in the limit of small avoided crossing energy gap. Although these approaches have had some success, each method is applicable only in very specific regions of parameter space, and the results thus give a patchwork analytical understanding of LMSZ interferometry. As a consequence, much of the structure underlying the diverse interference patterns that arise in LMSZ interferometry has gone overlooked and unappreciated although it provides important insight into the relevant quantum dynamics.

In this Letter, we propose a general framework based on Floquet theory that can extract the LMSZ interference patterns without any approximations to the driving field or Hamiltonian and without solving the Schrödinger equation. We instead exploit the fact that the interference patterns of LMSZ experiments are intimately related to periodic evolution of the system. Constraining the evolution to be periodic leads to a condition on the Hamiltonian parameters; the parameter values that satisfy this condition give the locations of resonances in the LMSZ interference pattern. In particular, we establish that these special values of the parameters arise as the zeros of a certain infinite Floquet determinant (FD). Remarkably, these zeros trace the interference pattern exactly, and in the process provide a deeper understanding of the origin and nature of LMSZ resonances.

The advantages of this approach are twofold. First, we can exactly reconstruct the interference pattern for experimentally relevant driving fields by simply diagonalizing matrices, and for the typical case of monochromatic driving, these matrices have the additional advantage of being tridiagonal, greatly simplifying the diagonalization process. Secondly, this method distinguishes three different classes of resonances, a fundamental aspect of the resonance structure that has not been captured by

other approaches. We refer to these classes as “real,” “complex,” and “accidental” resonances. The real and complex resonances are universal features corresponding to quantum evolution that is periodic regardless of the initial conditions; i.e., the system “resonates” at the driving frequency; these resonances are completely characterized by the zeros of the FD. On the other hand the accidental resonances correspond to nonperiodic evolution depend on the initial conditions of the system, and are characterized by both the FD zeros and a set of nonuniversal eigenvectors. Every resonance that occurs in LMSZ interferometry belongs to one of these three resonance classes.

Resonance classes.—Two-level LMSZ interferometry is described by the following Hamiltonian:

$$H = J(t)\sigma_z + h\sigma_x, \quad (1)$$

where σ_z and σ_x are Pauli matrices, $J(t+T) = J(t)$ is a periodic drive field with frequency ω and period $T = 2\pi/\omega$, and the constant $2h$ is the minimal energy gap of the avoided crossing (centered at $J = 0$) formed between the two diabatic levels, which we label $|1\rangle$ and $|2\rangle$. In qualitative descriptions of LMSZ interferometry, an analogy with a Mach-Zehnder interferometer is sometimes drawn [17]. Our study of LMSZ interference patterns focuses specifically on the probability that the driving field evolves the system from state $|1\rangle$ at $t = 0$ to state $|2\rangle$ at $t = nT$, corresponding to $2n$ complete traversals through the avoided crossing. We parametrize the evolution operator generated by Hamiltonian (1) as

$$U = \begin{pmatrix} u_{11} & -u_{21}^* \\ u_{21} & u_{11}^* \end{pmatrix}, \quad (2)$$

with $u_{11}(0) = 1$, $u_{21}(0) = 0$, and $|u_{11}|^2 + |u_{21}|^2 = 1$. The probability to be in state $|2\rangle$ after one drive period is $P_2(T) \equiv |u_{21}(T)|^2$, while after n drive periods it is

$$P_2(nT) = \frac{\sin^2[n\cos^{-1}(\text{Re}[u_{11}(T)])]}{1 - \text{Re}[u_{11}(T)]^2} P_2(T). \quad (3)$$

To describe experiments in which the final state probability is averaged over many drive periods, we also consider the quantity $\bar{P}_2(nT) \equiv (1/n) \sum_{m=1}^n P_2(mT)$. For certain values of the drive field parameters and h , $P_2(T)$ [and hence $P_2(nT)$ and $\bar{P}_2(nT)$] vanish; we refer to this point in parameter space as a resonance (also referred to as coherent destruction of tunneling [16,34]). The collection of all such resonances forms an interference pattern. An example of such an interference pattern is shown in the left panel of Fig. 1. Basic Floquet theory states that the evolution operator for a periodic Hamiltonian can be expressed as [32]

$$U = \begin{pmatrix} p_{11} & -p_{21}^* \\ p_{21} & p_{11}^* \end{pmatrix} \begin{pmatrix} e^{-iEt} & 0 \\ 0 & e^{iEt} \end{pmatrix} \begin{pmatrix} p_{11}^*(0) & p_{21}^*(0) \\ -p_{21}(0) & p_{11}(0) \end{pmatrix}, \quad (4)$$

where $p_{11}(t+T) = p_{11}(t)$, $p_{21}(t+T) = p_{21}(t)$ are periodic functions with $|p_{11}|^2 + |p_{21}|^2 = 1$, and E is the

quasienergy. It is clear from this equation that the evolution is periodic only if $E = k\pi/T$ for some integer k . When k is odd, the state acquires an overall minus sign at $t = T$; while this minus sign is immaterial for a system with only two levels, it can be relevant when additional levels are present. Therefore we maintain a distinction between 2π - and 4π -periodic evolutions arising when $k = 0$ or $k = 1$, respectively. Equating Eqs. (2) and (4) gives the functions u_{11} and u_{21} after one full period,

$$\begin{aligned} u_{11}(T) &= e^{iET} - 2i|p_{11}(0)|^2 \sin(ET), \\ u_{21}(T) &= -2ip_{11}^*(0)p_{21}(0) \sin(ET). \end{aligned} \quad (5)$$

These expressions make it clear that $P_2(T)$ can only vanish if $E = k\pi/T$, i.e. if the evolution is 2π or 4π periodic, or if $p_{11}^*(0)p_{21}(0) = 0$, in which cases the evolution is generally not periodic. Thus we see that the resonances naturally divide into two classes: resonances that satisfy $E = k\pi/T$ and correspond to periodic evolution, and resonances that obey the condition $p_{11}^*(0)p_{21}(0) = 0$ and correspond to nonperiodic evolution. Resonances of the latter type will be referred to as accidental resonances. We show below that the resonances associated with periodic evolution can be further categorized into real and complex resonances, corresponding to real and complex roots of the FD. In the rare case where both $E = k\pi/T$ and $p_{11}^*(0)p_{21}(0) = 0$ hold, the resonance will be classified as real.

To our knowledge, the distinction between the different types of LMSZ resonances has not previously been identified in the literature. It is important to make this distinction because these classes have different experimental manifestations. Real and complex resonances are universal features in the sense that they are determined solely by the quasienergy, whereas accidental resonances are nonuniversal since they depend on the initial data $p_{11}^*(0)$, $p_{21}(0)$. Real and complex resonances occur when the evolution of the system is periodic; the system is rotated by 2π or 4π about some axis. Accidental resonances do not generally correspond to periodic evolution. Instead, they correspond simply to a process in which the state is rotated partially about the drive axis. As shown below in the case of monochromatic driving, accidental resonances depend on the phase of the drive field and will thus be washed out in experiments that are insensitive to this phase. On the other hand, real and complex resonances are less visible after averaging over many periods.

Floquet determinant.—The fact that real and complex resonances are associated with special values of the quasienergy means that we do not need to solve the quantum evolution in order to compute the parameter values where these resonances occur. However, in order to see this, it helps to first set up a formal series solution for this evolution even though we do not need to compute this solution explicitly. For this purpose, instead of u_{11} and u_{21} , it is convenient to work with the functions

$$\phi_1 = e^{-i \int_0^t dt' J(t')} p_{21} e^{-iEt}, \quad \phi_2 = e^{-i \int_0^t dt' J(t')} p_{11}^* e^{iEt}, \quad (6)$$

which are independent solutions of the following second-order Schrödinger equation:

$$\ddot{\phi} + 2iJ\dot{\phi} + h^2\phi = 0. \quad (7)$$

The motivation for introducing ϕ_1 and ϕ_2 is that since J , p_{11} , and p_{21} are each periodic functions, ϕ_1 and ϕ_2 admit Fourier series expansions,

$$\phi_1 = \sum_{m=-\infty}^{\infty} a_m e^{i(m+\alpha_+)\omega t}, \quad \phi_2 = \sum_{m=-\infty}^{\infty} b_m e^{i(m+\alpha_-)\omega t}, \quad (8)$$

where $\alpha_{\pm} = (\mp E - \epsilon)/\omega$, and we have allowed for a possible overall additive constant ϵ in $J(t)$ such that $\int_0^T dt' J(t') = \epsilon T$. We may think of ϵ as a drive field detuning parameter. Plugging these expansions into the Schrödinger equation (7) along with a similar expansion for the drive field $J = \sum_m j_m e^{im\omega t}$, we obtain a recursion relation for the Fourier coefficients,

$$2\omega \sum_{\ell} j_{m-\ell} (\ell + \alpha_+) a_{\ell} + [\omega^2 (m + \alpha_+)^2 - h^2] a_m = 0, \quad (9)$$

and similarly for b_m with $\alpha_+ \rightarrow \alpha_-$. We can organize the coefficients in this recursion relation into an infinite matrix M_+ which acts on the infinite vector $a \equiv (\dots, a_{m-1}, a_m, a_{m+1}, \dots)$, recasting Eq. (9) as the condition that a is a null vector of M_+ : $M_+ a = 0$. Similarly, $b \equiv (\dots, b_{m-1}, b_m, b_{m+1}, \dots)$ is a null vector of a matrix M_- . For generic Hamiltonian parameters, the null spaces of M_+ and M_- must both be nonempty for some value of E since the Schrödinger equation always has a solution. Since a nonempty null space implies the vanishing of the determinant, if we impose the periodicity condition $E = k\pi/T$, we obtain a general formula for the locations of real and complex resonances,

$$\det M_k = 0, \quad (10)$$

where $M_k \equiv M_+(\alpha_+ = -k/2 - \epsilon/\omega)$. We refer to $\det M_k$ as a Floquet determinant. Equation (10) is one of the main results of this Letter. Given a periodic drive field $J(t)$ with frequency ω and detuning ϵ , we can systematically construct the matrix M_k , which depends only on drive parameters and the energy gap h . A set of parameters which solves Eq. (10), i.e., a root of the FD, corresponds to the location of a resonance in the LMSZ interference pattern, with real and complex roots giving real and complex resonances, respectively. Physical solutions are of course given by real parameter values; however, the real parts of complex roots with small imaginary parts still give the locations of approximate resonances. Note that it suffices to solve Eq. (10) only for the cases $k = 0$ and $k = 1$ in order to obtain the full set of resonances in the interference pattern.

Other choices of k are equivalent to these since the recursion relation (9) is invariant under a shift of k by an even integer. Also note that we do not need to separately solve the condition (10) with α_+ replaced by α_- since $M_+ = M_- = M_k$ when $E = k\pi/T$. This degeneracy translates to a twofold degeneracy in the solutions of Eq. (10).

A further crucial point pertains to how one should solve Eq. (10). Notice that M_k is a linear function of both the driving field amplitude A (since the j_m are linear in A), and h^2 . This means that if we want to fix all other parameters and solve for either A or h^2 , we may do so by reinterpreting $M_k a = 0$ as either an ordinary (in the case of h^2) eigenvalue problem or as a generalized (in the case of A) eigenvalue problem. For instance, if we wish to fix all driving field parameters and solve for the values of h that correspond to real or complex resonances, we should rewrite the null space condition $M_k a = 0$ as $M_k^{h=0} a = h^2 a$, so that the resonances are given by the eigenvalues of $M_k^{h=0}$. In practice, we must truncate the infinite matrix M_k in order to solve this eigenvalue problem, and the issue of convergence with respect to truncation size becomes important. We comment on this further in the specific case of monochromatic driving presented below.

Monochromatic driving.—We illustrate the general analysis given above with the example of monochromatic driving, which is a common choice in LMSZ interferometry experiments (see, e.g., Ref. [16]),

$$J(t) = \epsilon + A \sin(\omega t + \varphi). \quad (11)$$

The matrix M_k for this driving field is given in the Supplemental Material [35]. As described above, we fix all parameters except for A and solve $\det M_k = 0$, treating A as the generalized eigenvalue to be computed. As a representative example we fix $h = 5\omega$, scan ϵ , and solve for A for both $k = 0$ and $k = 1$. Convergence with respect to the truncation size N of M_k is very rapid, with full convergence of the eigenvalues $A < A_{\max}$ occurring roughly for $N \geq 4A_{\max}$. Eigenvalues larger than A_{\max} gradually become inaccurate due to the truncation. In Fig. 1, we overlay the resulting roots on the interference pattern obtained by solving the Schrödinger equation numerically, directly demonstrating that the FD roots accurately trace the contours of resonances for all values of ϵ . In Fig. 2, we show a slice of the interference pattern with $\epsilon = \omega$. Remarkably, all the resonance points evident in the numerical curve are exactly captured by the characteristic values of A . Moreover, it is clear from the figure that for smaller driving amplitudes, the resonances alternate between real and complex (corresponding to 2π and 4π periodicity, respectively), while for larger amplitudes, all the resonances are real. We admit complex resonances with imaginary part less than 10^{-2} . The fact that real resonances are singled out at larger amplitudes can be understood from the fact that in this regime, the energy gap h can be neglected relative to the driving amplitude, and the

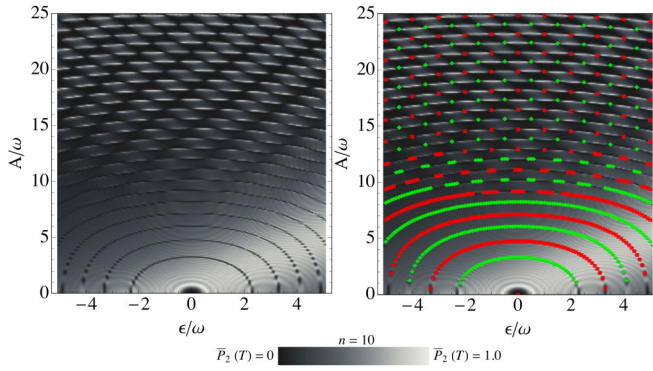


FIG. 1 (color online). Left: $P_2(nT)$ with $n = 10$ as a function of drive amplitude A and detuning ϵ for monochromatic driving from numerical solution of Schrödinger equation with $\varphi = -\pi/2$, and $h = 5\omega$. Right: red squares and green diamonds mark real and complex roots of FD, respectively.

quasienergy is simply given by the detuning $E = \pm\epsilon$. For the example shown in Fig. 2, ϵ is an integer, so that only resonances corresponding to integer values of the quasienergy, namely the 2π -periodic resonances, appear. This argument also reveals that no real or complex resonances occur at large amplitude when 2ϵ is not an integer, a fact which is evident in the right panel of Fig. 1. The alternating behavior at lower amplitude can be traced to the alternating integer and half integer eigenvalues of the harmonic oscillator, which coincides with the monochromatic driving Hamiltonian in the limit $\hbar^2 \gg A$. Figure 2 shows a slice of the resonance pattern after one traversal through the avoided crossing; in experiments where the final state probability is averaged over many periods, most of the resonances remain robust and visible despite this averaging, while a few either become sharper or disappear altogether (see the Supplemental Material [35]). The general robustness of LMSZ resonances is particularly important for their experimental observability.

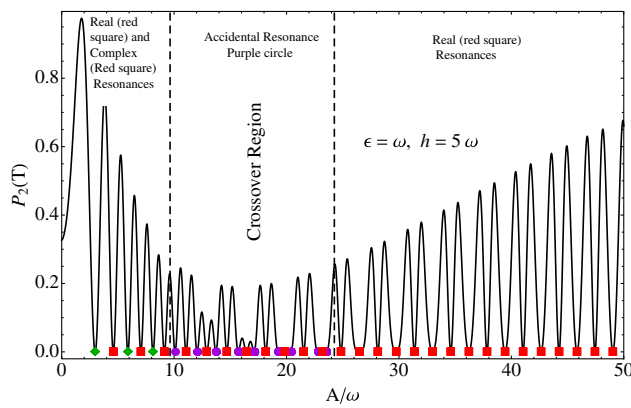


FIG. 2 (color online). $P_2(T)$ from numerical solution with $h = 5\omega$, $\epsilon = \omega$, $\varphi = -\pi/2$. Red squares, green diamonds, and purple circles mark real, complex, and accidental resonances obtained from the FD, respectively.

Accidental resonances.—In addition to real and complex resonances, the FD method can also capture the interesting class of accidental resonances (AR). When the system is tuned to an accidental resonance, the probability to be in the excited state $P_2(T)$ vanishes even though the evolution is not periodic. The defining criterion for ARs, $p_{11}^*(0)p_{21}(0) = 0$, can be reexpressed as the condition that the sum of the components of one of the null vectors a or b vanishes: $(\sum_{\ell} a_{\ell})(\sum_m b_m) = 0$. Unlike the cases of real and complex resonances, the quasienergy associated with an AR can have any value. However, since the quasienergy is only defined modulo integer multiples of ω , all the ARs can be obtained by scanning over $0 \leq E < \omega$, solving the FD in each case, and keeping those resonances that satisfy $\sum_m a_m = 0$ or $\sum_m b_m = 0$. Figure 3 shows the ARs that result from this method along with FD results for real and complex resonances for a particular set of parameters, illustrating that all the resonances are captured by the FD method. It is typically the case that the conditions $\sum_m a_m = 0$ and $\sum_m b_m = 0$ are satisfied only approximately, in which case it is necessary to introduce a small upper cutoff (of the order $|\sum_m a_m| < 10^{-2}$) on the sums of a_m and b_m in order to compute approximate ARs. In Fig. 3, we note that for smaller values of A , resonances are either real or complex, while for larger values of A all resonances are accidental, implying a crossover region where real or complex resonances are converted to accidental resonances. Figure 4 shows the same density plot of Fig. 1 but in a region of larger drive amplitude. The figure reveals that this conversion process happens for any noninteger value of 2ϵ , while for integer values, the resonances remain real or complex beyond the crossover region. In other words, when the detuning is set to one of these special values, the evolution at the resonances remains (anti)periodic as the drive amplitude is increased, whereas for more generic detunings, the evolution invariably becomes nonperiodic at larger amplitudes.

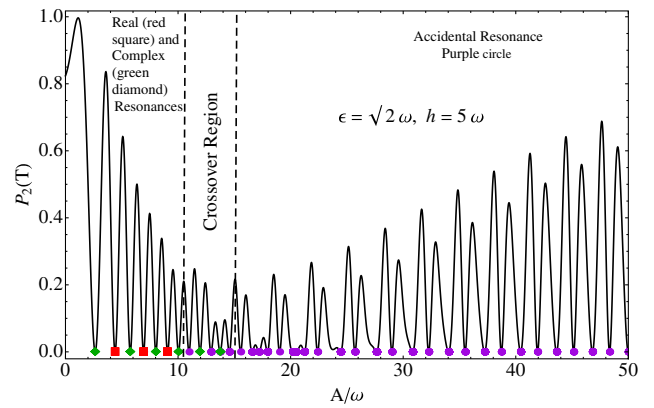


FIG. 3 (color online). $P_2(T)$ from numerical solution with $h = 5\omega$, $\epsilon = \sqrt{2}\omega$, $\varphi = -\pi/2$. Red squares, green diamonds, and purple circles mark real, complex, and accidental resonances obtained from the FD, respectively.

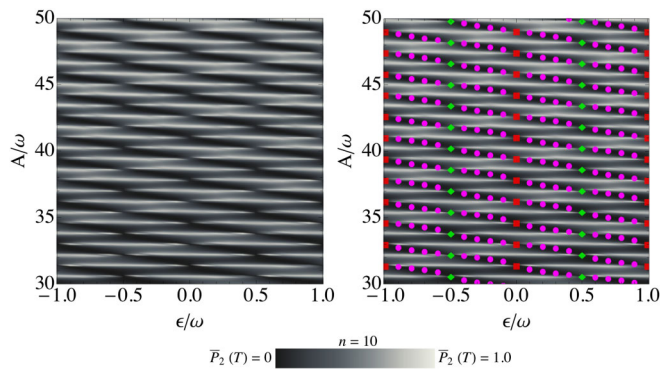


FIG. 4 (color online). $P_2(T)$ as a function of A and ϵ for the parameters of Fig. 1. Real (red squares) and complex (green diamonds) resonances only occur for $2\epsilon/\omega = \text{integer}$, while accidental (purple circles) resonances occur for nonintegral values of 2ϵ .

Conclusion.—We have presented a general framework using Floquet determinants for classifying the resonance structure of LMSZ interferometry into three basic categories distinguished by whether these resonances correspond to periodic or nonperiodic quantum evolution. Our approach applies to all parameter regimes, giving a unified picture of LMSZ interferometry.

We thank Lev Bishop and Benjamin Fregoso for helpful discussions. This work is supported by LPS-NSA, IARPA, and JQI-NSF-PFC.

- [1] L. Landau, *Phys. Z. Sowjetunion* **2**, 46 (1932).
- [2] C. Zener, *Proc. R. Soc. A* **137**, 696 (1932).
- [3] E. C. G. Stückelberg, *Helv. Phys. Acta* **5**, 369 (1932).
- [4] E. Majorana, *Nuovo Cimento* **9**, 43 (1932).
- [5] S. Shevchenko, S. Ashhab, and F. Nori, *Phys. Rep.* **492**, 1 (2010).
- [6] M. C. Baruch and T. F. Gallagher, *Phys. Rev. Lett.* **68**, 3515 (1992).
- [7] S. Yoakum, L. Sirko, and P. M. Koch, *Phys. Rev. Lett.* **69**, 1919 (1992).
- [8] J. Q. You and F. Nori, *Nature (London)* **474**, 589 (2011).
- [9] L. Childress and J. McIntyre, *Phys. Rev. A* **82**, 033839 (2010).
- [10] G. D. Fuchs, G. Burkard, P. V. Klimov, and D. D. Awschalom, *Nat. Phys.* **7**, 789 (2011).
- [11] J. Zhang, J. H. Shim, I. Niemeyer, T. Taniguchi, T. Teraji, H. Abe, S. Onoda, T. Yamamoto, T. Ohshima, J. Isoya, and D. Suter, *Phys. Rev. Lett.* **110**, 240501 (2013).
- [12] J. R. Petta, H. Lu, and A. C. Gossard, *Science* **327**, 669 (2010).
- [13] L. Gaudreau, G. Granger, A. Kam, G. C. Aers, S. A. Studenikin, P. Zawadzki, M. Pioro-Ladriere, Z. R. Wasilewski, and A. S. Sachrajda, *Nat. Phys.* **8**, 54 (2011).
- [14] H. Ribeiro, G. Burkard, J. R. Petta, H. Lu, and A. C. Gossard, *Phys. Rev. Lett.* **110**, 086804 (2013).
- [15] H. Ribeiro, J. R. Petta, and G. Burkard, *Phys. Rev. B* **87**, 235318 (2013).
- [16] J. Stehlik, Y. Dovzhenko, J. R. Petta, J. R. Johansson, F. Nori, H. Lu, and A. C. Gossard, *Phys. Rev. B* **86**, 121303 (R) (2012).
- [17] W. D. Oliver, Y. Yu, J. C. Lee, K. K. Berggren, L. S. Levitov, and T. P. Orlando, *Science* **310**, 1653 (2005).
- [18] D. M. Berns, M. S. Rudner, S. O. Valenzuela, K. K. Berggren, W. D. Oliver, L. S. Levitov, and T. P. Orlando, *Nature (London)* **455**, 51 (2008).
- [19] C. M. Quintana, K. D. Petersson, L. W. McFaul, S. J. Srinivasan, A. A. Houck, and J. R. Petta, *Phys. Rev. Lett.* **110**, 173603 (2013).
- [20] B. Damski and W. H. Zurek, *Phys. Rev. A* **73**, 063405 (2006).
- [21] S. Ashhab, J. R. Johansson, A. M. Zagoskin, and F. Nori, *Phys. Rev. A* **75**, 063414 (2007).
- [22] M. S. Rudner, A. V. Shytov, L. S. Levitov, D. M. Berns, W. D. Oliver, S. O. Valenzuela, and T. P. Orlando, *Phys. Rev. Lett.* **101**, 190502 (2008).
- [23] M. V. Berry, *J. Phys. A* **42**, 365303 (2009).
- [24] S.-K. Son, S. Han, and Shih-I Chu, *Phys. Rev. A* **79**, 032301 (2009).
- [25] A. Ruschhaupt, X. Chen, D. Alonso, and J. G. Muga, *New J. Phys.* **14**, 093040 (2012).
- [26] N. Malossi, M. G. Bason, M. Viteau, E. Arimondo, R. Mannella, O. Morsch, and D. Ciampini, *Phys. Rev. D* **87**, 012116 (2013).
- [27] J.-N. Zhang, C.-P. Sun, S. Yi, and F. Nori, *Phys. Rev. A* **83**, 033614 (2011).
- [28] A. M. Satanin, M. V. Denisenko, S. Ashhab, and F. Nori, *Phys. Rev. B* **85**, 184524 (2012).
- [29] Z. Sun, J. Ma, X. Wang, and F. Nori, *Phys. Rev. A* **86**, 012107 (2012).
- [30] S. N. Shevchenko, S. Ashhab, and F. Nori, *Phys. Rev. B* **85**, 094502 (2012).
- [31] A. M. Satanin, M. V. Denisenko, A. I. Gelman, and F. Nori, *arXiv:1305.4800*.
- [32] J. Shirley, *Phys. Rev.* **B138**, 979 (1965).
- [33] C. E. Creffield, *Phys. Rev. B* **67**, 165301 (2003).
- [34] F. Grossmann, T. Dittrich, P. Jung, and P. Hänggi, *Phys. Rev. Lett.* **67**, 516 (1991).
- [35] See Supplemental Material at <http://link.aps.org/supplemental/10.1103/PhysRevLett.111.130405> for further details of monochromatic driving and experimental observability of resonances.